BBA - Molecular Basis of Disease 1867 (2021) 166048

Contents lists available at ScienceDirect

BBA - Molecular Basis of Disease

journal homepage: www.elsevier.com/locate/bbadis

PKC epsilon as a neonatal target to correct FXS-linked AMPA receptor translocation in the hippocampus, boost PVN oxytocin expression, and normalize adult behavior in *Fmr1* knockout mice

Alexandra Marsillo [a], Lovena David [d], Bishoy Gerges [d], Daniel Kerr [d], Rodina Sadek [d], Vitaliy Lasiychuk [d], David Salame [d], Youstina Soliman [d], Silvia Menkes [d], Aheli Chatterjee [d], Andrew Mancuso [b], Probal Banerjee [a,c,d,*]

[a] CUNY Doctoral Programs in Biology, The College of Staten Island (CUNY), Staten Island, NY 10314-6609, United States of America
[b] CUNY Doctoral Programs in Biochemistry, The College of Staten Island (CUNY), Staten Island, NY 10314-6609, United States of America
[c] Department of Chemistry, The College of Staten Island (CUNY), Staten Island, NY 10314-6609, United States of America
[d] Center for Developmental Neuroscience, The College of Staten Island (CUNY), Staten Island, NY 10314-6609, United States of America

ARTICLE INFO

Keywords:
Fmr1
PKCε
GluR2
Hippocampus
Hypothalamus
Oxytocin

ABSTRACT

Fragile X Syndrome (FXS) is an inherited developmental disorder caused by the non-expression of the *Fmr1* gene. FXS is associated with abnormal social and anxiety behavior that is more prominent among males. Given that oxytocin (OXT) regulates both social and anxiety behavior, we studied the effect of FXS in the hypothalamic paraventricular nucleus (PVN), the major central source of OXT. We observed a significant suppression of protein kinase C epsilon (PKCε) (34%) in the ventral hippocampal CA1 region of postnatal day-18 (P18) male *Fmr1* knockout (KO) mice, which displayed social behavior deficits and hyper-anxiety in adulthood. These mice also displayed a 39% increase in cell surface α-amino-3-hydroxy-5-methyl-4-isoxazolepropionic acid (AMPA) receptor (AMPAR) at P18 (measured by the surface level of the AMPAR subunit GluR2), thereby indicating excitation of the CA1 neurons. It is known that neuronal activation at CA1 is linked to an inhibition of the PVN neurons. As expected, these mice also displayed a 25% suppression of oxytocin+ (OXT+) cells in the PVN at P20. Stimulating PKCε during postnatal days 6–,14 (P6–14) mice using a selective activator, dicyclopropyl-linoleic acid (DCP-LA), corrected AMPAR externalization in CA1 and suppression of OXT+ cell number in PVN in a PKCε dependent manner. Most notably, neonatal DCP-LA treatment rescued social behavior deficits and hyper-anxiety, displayed by adult (≥P60) male but not female KO mice. Thus, neonatal stimulation of PKCε could be a strategy to correct endophenotypic anomalies during brain development and aberrant adult behavior of the FXS males to the wild-type levels.

1. Introduction

Fragile X Syndrome (FXS) is a complex neuro-developmental disorder resulting from mutation of the *Fmr1* gene on the X chromosome, and subsequent loss of its protein product, the neuronal translational regulator FMRP [1,2]. At its core, FXS is characterized by a pervasive central synaptopathy, manifesting as a broad range of neurological and behavioral symptoms [3,4]. Although FXS is the most common cause of monogenic autism and inherited mental retardation [5,6], no single effective treatment for the disorder exists. While group 1 metabotropic glutamate receptor antagonists had demonstrated promise in early stages of research, they have so far failed to improve symptoms beyond placebos in double-blinded clinical trials [7]. Thus, the need for effective treatments for FXS remains imperative.

Abbreviations: Fmr1, Fragile X mental retardation 1 gene; FMRP, Fragile X mental retardation protein; FXS, Fragile X Syndrome; WT, Wild-type; KO, Knock-out; AMPA, α-amino-3-hydroxy-5-methyl-4-isoxazolepropionic acid receptor; GluR2, Glutamate receptor 2 subunit of the AMPA receptor; mGlur, Metabotropic glutamate receptor; Myr-εV1-2, N-Myr-EAVSLKPT (a selective PKCε translocation inhibitor); DCP-LA, 8-[2-(2-pentyl-cyclopropylmethyl)-cyclopropyl]-octanoic acid (a selective stimulator of PKCε); OXT, Oxytocin; BNST, Bed Nucleus of the Stria Terminalis..

* Corresponding author at: Department of Chemistry and Center for Developmental Neuroscience, The City University of New York at The College of Staten Island, Staten Island, NY 10314, United States of America.
E-mail address: probal.banerjee@csi.cuny.edu (P. Banerjee).

https://doi.org/10.1016/j.bbadis.2020.166048
Received 19 August 2020; Received in revised form 19 November 2020; Accepted 14 December 2020
Available online 23 December 2020
0925-4439/© 2020 Elsevier B.V. All rights reserved.

It is estimated that 70% of males and 56% of females with FXS are co-diagnosed with an anxiety disorder [8,9]. Moreover, many symptoms of FXS are attributed to anxiety, including deficits in social interaction and communication. For instance, while FXS patients are often deeply desirous of human interaction, they tend to avoid social situations due to severe social anxiety [10,11]. The central oxytocinergic system is well established as an important regulator of social behavior, anxiety levels, and stress coping [12]. Thus, it is likely that the oxytocinergic system is compromised in FXS. However, only a few studies have investigated this possibility. Exogenous administration of oxytocin (OXT) has shown some promise in patients with FXS [13], but its efficacy as a treatment for autistic-like behavior remains controversial [14], and some studies have failed to show an effect [15–17]. In light of this information, we postulate that identifying and correcting FXS-associated changes within the endogenous oxytocinergic system during early brain development may be effective in eliminating the later-life behavioral deficits.

Circuit hyper-excitability is a well-known phenomenon associated with FXS [18], with epilepsy occurring in 10–20% of patients [19,20]. It has long been suspected that the hippocampus may be one such locus of hyper-excitability. This may be particularly relevant to the pathogenesis of FXS since the hippocampus is a hub, which regulates the activity of a number of downstream structures relevant to behavior, including the cortex, amygdala, and the hypothalamic paraventricular nucleus (PVN). Thus, inappropriate hippocampal activity at a young age may lead to aberrant brain wiring between these structures that may later manifest as behavioral anomalies.

Here, we report that *FVBPde*^{WT} *Fmr1* KO mice harbor significantly suppressed PKCε (an Fmrp target [21]) than *FVBPde*^{WT} (Wild type) mice in the CA1 neurons at P18 and this is associated with externalized α-amino-3-hydroxy-5-methyl-4-isoxazolepropionic acid (AMPA) receptor (AMPA-R) molecules at CA1 pyramidal neuron synapses even in the basal state, potentially leading to hyper-excitability. This putatively excited state of the CA1 neurons is associated with an inhibition of OXT expression within the PVN in the KO mice at P20, explaining the altered social and anxiety behavior in this mouse model in adulthood. Quite strikingly, we could reverse the suppressed OXT expression and aberrant behaviors through neonatal treatment with a selective PKCε activator, dicyclopropyl-linoleic acid (DCP-LA). Thus, targeting PKCε-mediated signaling during the early postnatal stage may represent a novel treatment strategy for FXS. Our mechanistic analysis may lend support to other studies demonstrating that bryostatin, a PKCε stimulator, is capable of correcting structural abnormalities in hippocampal dendritic spines and rescuing spatial learning and memory in juvenile *Fmr1* KO mice [22].

2. Materials and methods

2.1. Animals

Mice (*FVB.129P2-Pde6b+*) (mentioned here as *FVBPde*^{WT} or *FVBPde*) with the wild-type (WT) or *Fmr1* knockout (KO) allele were originally obtained from The Jackson Laboratory, housed in the College of Staten Island (CSI) Animal Care Facility, provided food and water *ad libitum*, and handled in accordance with CUNY-IACUC approved procedures. Once obtained from The Jackson Laboratory, the WT and KO animals were bred separately and all our experiments were performed within the F3 generation. Following this, the KO females were backcrossed with WT males to obtain *Fmr1* heterozygous females and hemizygous males, which were identified by genotyping using PCR primer sequences provided by The Jackson Laboratory: KO-forward: 5′-CAC GAG ACT AGT GAG ACG TG-3′; WT-reverse: WT-forward: 5′-TGT GAT AGA ATA TGC AGC ATG TGA-3′; Common-reverse: 5′-CTT CTG GCA CCT CCA GCT T-3′. All three primers were used together for PCR to obtain 400-bp and 131-bp products for KO and WT respectively. The heterozygous females yielded both PCR bands. The *Fmr1(−/y)* (hemizygous) males and *Fmr1 (+/−)* (heterozygous) females were then paired to obtain *Fmr1(−/−)* females and *Fmr1(−/y)* males, which were named as KO females and males respectively. The KO mice were paired to generate the F1-F3 generations. The wild type (WT) control mice were obtained by pairing *FVBPde* male mice with the *Fmr1(+/−)* females. Each experiment included Vehicle- and DCP-LA-treated (3 mg/kg) *Fmr1(−/−)* females and *Fmr1(−/y)* male mice from the same generation as of wild type (WT) progenies obtained by pairing *FVBPde* males with *FVBPdeFmr1 (+/−)* females. Data were obtained from multiple litters of the F1 to F3 generations and then combined to obtain the results presented in this article.

The behavioral anomalies were observed only in the KO males but not in the KO females. Based on this information, our molecular analyses were conducted only with the WT and KO males.

2.2. Drug treatments

Since the linoleic acid analog DCP-LA is known to cross the blood-brain barrier and is stable *in vivo* [23,24], administration of DCP-LA was conducted intra-peritoneally (i.p.). *Fmr1* KO littermates were injected intraperitoneally with 3 mg/kg DCP-LA or vehicle at P6, P10, and P14. Based on the average body weights of pups at P6, 10, and 14, aliquots of a 1 mg/ml DCP-LA solution in 95% 10 mM phosphate buffered saline (PBS), 5% DMSO (working stock) were injected i.p. into each pup to achieve a final concentration of 3 mg/kg of body weight for DCP-LA, and a final systemic DMSO concentration of <1%. WT controls were similarly injected with vehicle at the same time points (PBS containing the same concentration of DMSO). For studies involving the use of the selective PKCε inhibitor, Myr-εV1-2 (N-Myr-EAVSLKPT) (a.k.a. Myr-εV1/2), the peptide was prepared by solid-phase synthesis as reported earlier [25]. The peptide was then dissolved in the aforementioned DCP-LA working stock to achieve a final dosage of 50 μg/kg. The inhibitor was then injected (i.p.) simultaneously with 3 mg/kg DCP-LA at P6, P10, and P14. WT and KO controls were similarly injected with vehicle at the same time. To further ensure brain entry of the inhibitor, we additionally delivered Myr-εV1/2 (dissolved in vehicle) intra-nasally [26] at the aforementioned time-points, prior to the i.p. injections of DCP-LA. For each time point, we assumed an efficiency of 10% transfer across the olfactory epithelium and intranasally administered such a dose that would yield an intra-brain concentration of 0.1 μM of Myr-εV1/2. The total brain volume was determined by water displacement using brains isolated from other pups of the same age.

2.3. Immunohistochemistry

Mice were perfused trans-cardially with PBS, followed by 4% paraformaldehyde (PFA). The brains were fixed by overnight immersion in 4% PFA, then dehydrated overnight in 30% sucrose in PBS. Serial coronal slices of 30 μm thickness were obtained by cryosectioning and blocked overnight in 0.1% Triton X-100 and 10% serum obtained from the species used to raise the secondary antibody, in PBS. This was followed by treatment with the primary antibody in the same blocking solution overnight. To obtain a complete representation of the structures along the anterior-posterior axis, every 6th slice was used. For NeuN staining, the following antigen retrieval steps preceded blocking: 2 N HCl at 37 °C for 25 min, 1 N HCl at 0 °C for 10 min, neutralization with 0.1 M boric acid for 10 min, and then 3 rinses with PBS (10 min each). To study surface levels of GluR2, primary antibody targeting the extracellular N-terminus was used in conjunction with non-permeabilizing conditions (Triton X-100 and antigen retrieval omitted). The following primary antibodies were used: Mouse-anti NeuN, Millipore (1:500); Goat-anti GluR2 (N-19), Santa Cruz (1:1000); and Rabbit-anti Oxytocin, Immunostar (1:1000). Secondary antibodies used were Goat-anti mouse Alexa-Fluor 488, Goat-anti Rabbit Alexa-Fluor 568, and Rabbit-anti Goat Alexa-Fluor 568, Santa Cruz (1:500).

2.4. Western blotting

Hippocampal lysates were acutely acquired from P18 mice. The mice were sacrificed and brains were immediately submerged in oxygenated, ice-cold artificial cerebrospinal fluid (ACSF) containing 0.25 M sucrose. The brains were then sectioned into 300 μm thick slices using a Leica vibratome and incubated in the above solution. A 1.5 mm diameter biopsy hole-puncher was used to isolate the DG, CA3, and CA1 subregions of ventral hippocampi, as well as the PVN. The samples were then homogenized in RIPA buffer (PBS containing a complete protease inhibitor cocktail (Roche, Mannheim, Germany), 0.1 % SDS, 1% NP-40, 0.25% sodium deoxycholate, 1 mM sodium vanadate, 5 mM sodium fluoride, 50 mM sodium pyrophosphate, 3-mM PMSF and 3 mM EDTA) l and resolved by SDS-PAGE. The protein bands were then transferred to a nitrocellulose membrane, blocked in 3% BSA (for phosphorylated proteins) or 5% non-fat dry milk (for non-phosphorylated proteins) in 62.5 mM Tris-buffered saline (TBS) for 2 h at room temperature. The blots were then incubated with primary antibodies in the same blocking solution for 12 h at 4 °C and washed 3× with 62.5 mM Tris-gbuffreTBS containing 0.01% Tween (TTBS). Lastly, the blots were incubated with secondary antibodies (Goat anti-Rabbit IgG-HRP (1:50,000); Rabbit anti-Goat IgG HRP (1:20,000) and Goat anti-Mouse IgG-HRP (1:50,000), Santa Cruz, CA) for 2 h at room temperature, washed 3× with TTBS, and then developed using the SuperSignal West Pico Chemiluminescent Substrate kit for non-phosphorylated proteins or the SuperSignal West Dura kit (ThermoFisher) for phosphorylated proteins. Primary antibodies used were Rabbit-anti PKCε (C-15), Santa Cruz (1:1000); Goat-anti GluR2 (N-19), Santa Cruz (1:1000); Goat-anti phospho-GluR2 (Ser 880), Santa Cruz (1:1000); Rabbit anti GluR1, Immunostar (1:1000); Goat anti phospho-GluR1 (Ser 831), Santa Cruz (1:750); and Mouse-anti β-actin, Sigma (1:10,000). Secondary antibodies used were Goat anti-Rabbit IgG-HRP (1:50,000); Rabbit anti-Goat IgG HRP (1:20,000) and Goat anti-Mouse IgG-HRP (1:50,000), Santa Cruz.

2.5. Behavioral testing

All behavior testing was conducted in age- and sex- matched mice between P60 – P90. All behavior testing was conducted during the light phase. One hour prior to testing, the mice were transported to an adjacent anteroom to the behavior testing room and were acclimated in the dark for 1 h, allowing sufficient time for the animals to become active. During testing, the animals were recorded using an overhead camera. Additionally, a white noise generator was used to block out any extraneous noises that might cause distraction. After each trial, the apparatus was thoroughly cleaned with 70% ethanol in order to prevent odor cues left behind by the previous mouse. Captured videos were subsequently automatically analyzed using ANY-Maze motion-tracking software. For behaviors that could not be detected by ANY-Maze, the videos were scored manually while blinded to the treatment groups. Statistical analyses were carried out using unpaired, two-tailed *t*-test or analysis of variance (ANOVA). Significant main effects or interactions were followed up with *Tukey's HSD* (honestly significant difference) *post hoc* test. Data were presented as mean ± S.E.M. Statistical significance was defined as $p<0.05$.

2.6. Elevated-Plus Maze (EPM)

The EPM apparatus used consisted of two opposing open arms (36 cm × 7 cm) and two closed arms (36 cm × 7 cm), joined at a square central area (5 cm × 5 cm). The apparatus was constructed of wood with the maze floor covered with white-painted vinyl, which allowed sufficient traction for the mice to explore the maze comfortably while also providing sufficient contrast to detect their movements. The entire apparatus was elevated to a height of 50 cm above the floor by four supports beneath each arm. The open arms were illuminated at 70 lx and the closed arms were illuminated at ~10 lx by a central, overhead light. Mice were initially placed in the center of the maze, and the number of entries into the open arms and the time spent in the open arms and were subsequently measured over a period of 10 min.

2.7. Light-Dark Chamber (LDC) for anxiety measures

Designed based on the innate tendency of mice to hide in a dark chamber, the light-dark test was conducted according to published protocols with some modifications. The light-dark test apparatus consisted of a plastic box consisting of a 50 cm × 25 cm rectangular arena with 40 cm high walls, which was divided into two 25-cm compartments. The dark compartment was unlit (<5 lx), painted black with an opaque ceiling and walls, and the light compartment was transparent and illuminated by an overhead fluorescent tube (150 lx at cage floor). During the test, each mouse was placed in the center of the lit chamber and subsequently monitored for 10 min as it moved freely between the two chambers. The total number of transitions, the time spent in each chamber, and the latency to enter the light chamber was recorded manually by a blinded observer.

2.8. Social interaction test

Testing was conducted based on a previously-published protocol [27]. Testing took place in three sessions within a three-chambered box of standard dimensions, with openings between the chambers. After habituation to the empty box for 10 min, the subject was presented with the choice to investigate a stranger age- and sex-matched mouse under one pencil cup (target mouse) on one side of the apparatus, *versus* an empty pencil cup (novel object) on the opposite side of the apparatus, for 10 min. The time spent sniffing each pencil cup, the time spent in each chamber, and the number of entries into each chamber were measured. To avoid any potential biases toward one particular chamber, the positions of the target and novel object were switched between subjects. Sociability was defined as the subject mouse spending more time in the chamber containing a novel target mouse than in the chamber containing the inanimate novel object.

2.9. Statistical analysis

While comparing two data sets, two-tailed *t*-test with unequal variance was used. To compare among three or more sets, one-way ANOVA was used. Post-hoc analysis was performed using Tukey, and $p \leq 0.05$ was considered as significant.

3. Results

3.1. PKCε expression is suppressed in the Fmr1 KO ventral CA1 region

Darnell and colleagues have reported that FMRP binds to PKCε mRNA, presumably regulating its translation [21]. PKC has been shown to be essential for normal synaptogenesis, and modulates AMPA receptor surface localization *via* phosphorylation of the receptor's GluR1 and GluR2 subunits [28,29]. Given our previous observations that PKCε levels are higher than the other PKC isozymes in the hippocampus during the early postnatal period [30], we hypothesized that aberrant PKCε expression may potentially contribute in part to FXS pathogenesis.

The symptoms of FXS first become apparent within the first two years of human life, during which time sensory inputs play a key role in shaping brain wiring, and consequently, later-life behavior and emotional tone. Keeping this in mind, we studied hippocampal PKCε expression at both postnatal days 6 (P6), corresponding to birth in humans, and 18–20 (P18–20), corresponding to approximately 2 years of age in humans. Preliminary immunohistochemical analysis revealed high levels of PKCε expression throughout the ventral hippocampus at age P18, with localization in the soma and dendrites (Fig. S1-1). Whereas no difference in PKCε expression was observed between the WT

and KO groups at P6 (Fig. S1-2), we discovered significant suppression of PKCε expression in the ventral CA1 region at P18 (Fig. S1-1). This observation is particularly interesting because stimulation of ventral CA1 neurons has been shown to promote anxiety, whereas lesions to these same neurons produce an anxiolytic effect [31,32]. To confirm this finding, we performed western blot analysis on ventral CA1 lysates obtained from P18 pups. We observed a 34% decrease in ventral CA1 PKCε expression in the P18 KO pups, compared with WT controls (Fig. 1). Importantly, this time point occurs a few days after eye opening, at which point synaptogenesis dramatically surges in response to the influx of visual stimuli.

3.2. Suppression of PKCε is associated with altered AMPA receptor internalization in the juvenile Fmr1 KO ventral hippocampus

Taken together, these findings provide novel evidence that PKCε expression is altered during early postnatal brain maturation in two major brain regions relevant to social and emotional behavior in the *Fmr1* KO mouse model. To ascertain potential consequences of this reduced PKCε expression, we next investigated its involvement in AMPA receptor dynamics, as the AMPA receptor is a target of PKC-mediated signaling [28,29]. Most excitatory transmission in the brain is mediated by AMPA receptors, and dynamic alterations in the number of synapse-localized AMPA receptors is an important factor contributing to synaptic plasticity. Importantly, the subunit composition of the AMPA receptor is dependent on the brain region. During development, the majority of hippocampal AMPA receptors contain the GluR2 subunit, the expression of which is gradually up-regulated in the hippocampus from birth until adulthood. On the other hand, AMPA receptor subunit composition within the PVN is more heterogeneous, varying between different cell populations. Here, GluR2 is predominantly found in peripherally-releasing cells, whereas GluR1 is the major AMPA receptor subunit found in centrally-releasing, pre-autonomic cells [33].

Since PKCε expression was most significantly reduced in the ventral CA1 region of our *Fmr1* KO mice at P18 (Fig. S1-1), we honed in on this same region to examine GluR2 expression as a marker for the AMPA receptor. Interestingly, Western blot analysis did not detect any difference in total GluR2 expression between our WT and Fmr1 KO pups at P18 (Fig. 2A, middle row and C), which is consistent with the observation that GluR2 mRNA does not seem to be a target of FMRP [21]. Internalization of the AMPA receptor has been linked to PKC-mediated phosphorylation of the GluR2 subunit at serine 880 [28,29]. Intriguingly, we observed a 51% decrease in phosphorylated serine-880 GluR2 in these same lysates (Fig. 2A, top row and B), indicating that the process of AMPA receptor internalization may be disturbed.

In order to analyze surface levels of GluR2, we next performed immunohistochemical analysis of ventral hippocampal brain slices obtained from WT and *Fmr1* KO pups under non-permeabilizing conditions and using an N-terminal-directed antibody to selectively and accurately label surface GluR2. Confirming our hypothesis, a 39% increase in surface GluR2 (AMPA receptor) fluorescence in the P18 *Fmr1* KO CA1 area and a trend of increase in CA3 region were observed (Fig. 3). To investigate whether GluR2 serine-880 phosphorylation may be mediated by PKCε, we treated *Fmr1* KO pups with 3 mg/kg of the selective PKCε activator, dicyclopropyl-linoleic acid (DCP-LA), on P6. P10, and P14. Supporting our hypothesis, DCP-LA treatment was able to fully correct surface AMPA receptor levels at P18 in CA1 and CA3 neurons, and these mice were statistically indistinguishable from the WT group (Fig. 3).

The hippocampus, especially its ventral portion, is a hub that influences emotional behavior through its dense connections with the hypothalamus, amygdala, and cortex. With this information in mind, we next studied the paraventricular nucleus of the hypothalamus (PVN), which is the major central source of the pro-social and anxiolytic peptide, oxytocin (OXT). We first questioned if AMPA receptor dynamics might be altered in the PVN cells, where GluR1 is the predominant AMPA receptor subunit. The serine-831 residue of GluR1, like the serine 880 residue of GluR2, is subject to phosphorylation by PKC [34], but in this case, phosphorylation enhances the receptor's channel conductance [35]. However, we did not detect any difference in total GluR1 nor serine 831 phosphorylated GluR1 in WT *versus Fmr1* KO PVN lysate at P20 (Fig. 4A–C). Furthermore, we observed a significant increase in phospho-Ser880-GluR2 in the PVN of P20 KO males relative to WT, thus indicating a suppression of activity in P20 PVN neurons of the KO mice (Fig. 4D–F). However, PKCε levels were suppressed by 17% in the PVN (Fig. S4-1), which strongly indicated that the PVN-specific increase in phospho-Ser880-GluR2 was unlikely to be linked to a local PKCε-mediated phosphorylation in the PVN. Consistent with the increase in phospho-Ser880-GluR2, we observed a significant suppression of c-Fos expression in PVN of the P20 KO mice (Fig. 4G, H), thereby confirming a suppression of activity in these neurons.

3.3. PKCε-dependent reduction in the number of OXT-synthesizing PVN cells in juvenile Fmr1 KO mice

Given the number of neurobehavioral symptoms associated with FXS, we next explored the likely downstream contributions of the synaptic aberrations we have observed within the *Fmr1* KO hippocampus during the juvenile stage. The neuropeptide OXT is widely known to promote social behavior and temper anxiety levels [36–38]. Considering that many behavioral symptoms of FXS, including deficits in sociability, can stem from anxiety [39], it is likely that oxytocinergic signaling may be compromised in FXS [40]. As a potential mechanism, the hippocampus is known to inhibit the activity of the parvocellular division of the PVN of the hypothalamus *via* recruitment of GABA-ergic interneurons within the Bed Nucleus of the Stria Terminalis (BNST) [41,42]. A subset of parvocellular neurons within the PVN have been shown to produce centrally distributed OXT that has been linked to behavioral effects. Could hippocampal-exerted inhibition affect the OXT-producing neurons? Based on the knowledge that AMPA receptor externalization has been linked to higher excitatory drive [28,29], we suspect that the observed heightened surface AMPA receptor levels in the hippocampus may lead to a heightened inhibitory drive on the PVN.

To address this possibility, we first investigated whether OXT production was altered in the *Fmr1* KO brain relative to WT controls. We studied OXT expression at P20 (weaning age), at which point the PVN is fully developed, and allowing sufficient time for changes in the upstream ventral CA1 region to take effect. Immunohistochemical analysis

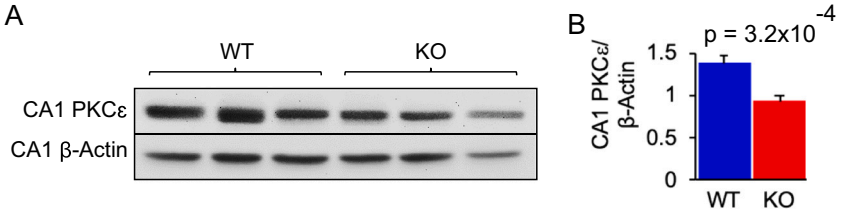


Fig. 1. PKCε expression is suppressed in the CA1 region of the hippocampus in the *Pde6b^{WT} Fmr1 KO* mice at P18. Lysates of tissue punches from the hippocampal CA1 regions of P18 WT and KO males were subjected to Western blotting. (A and B) The PKCε level was suppressed by 34% in the hippocampal CA1 region in *Fmr1* KO mice with respect to wild type (WT) (n = 6 for each group). As presented in Fig. S1-1, suppressed expression of PKCε in the CA1 region at P18 was also observed using immunohistochemistry. However, at P6, PKCε expression in the KO hippocampus was indistinguishable from that in the WT controls (Fig. S1-2).

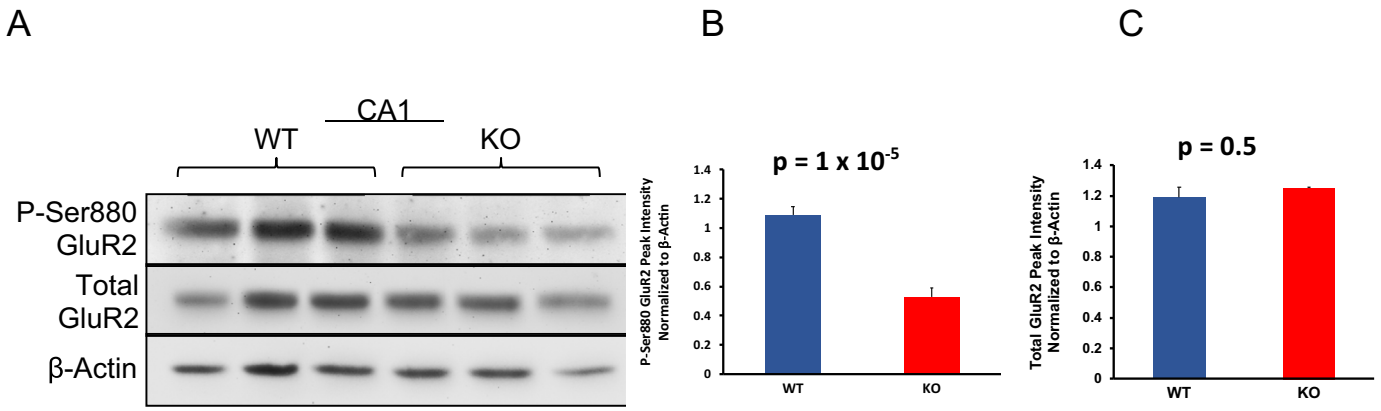


Fig. 2. Inactivating phosphorylation of the AMPA receptor GluR2 subunit is suppressed in the CA1 region in the *Pde6b*^{WT} *Fmr1 KO* mice at P18 with respect to WT (n = 6 for each group). Lysates hippocampal CA1 region were subjected to Western blotting to compare Phospho-Ser880-GluR2 levels between WT and KO male mice at P18. (A (top row) and B) A 51% suppression of Phospho-Ser880-GluR2 was observed in the KO mice relative to the WT. (A (Middle row) and C) The GluR2 levels were comparable between WT and KO (n = 6 for each group).

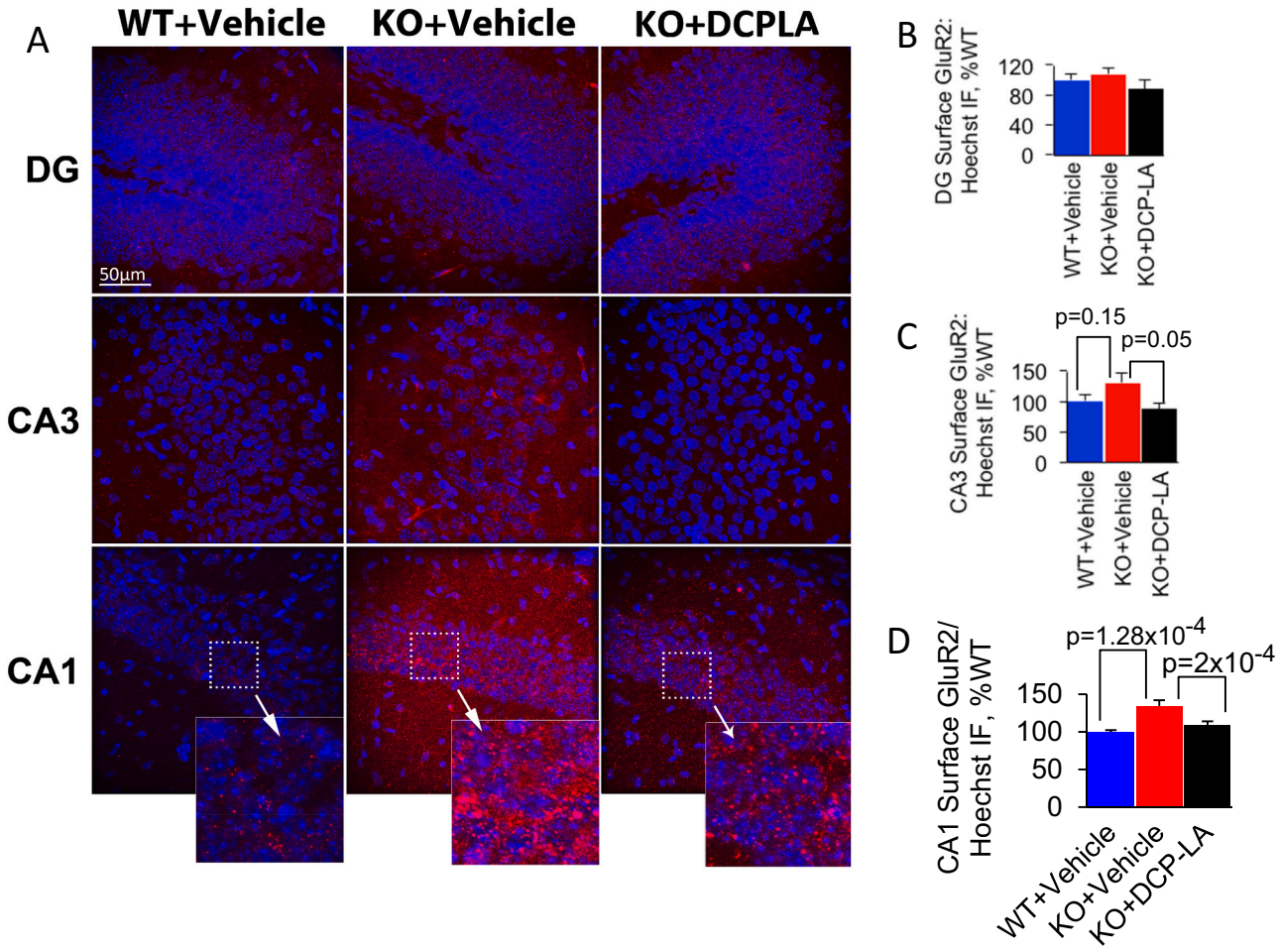


Fig. 3. Increased surface localization of the AMPA receptor in the CA1 neurons of the *Pde6b*^{WT} *Fmr1* KO mice at P18 relative to WT. (A and B) Hippocampal sections from WT, KO males treated with either vehicle or DCP-LA (3 mg/kg) on P6, 10, 14 were subjected to immunohistochemistry at P18 (without permeabilization) using an N-terminal-targeted GluR2 antibody to quantify surface expression of GluR2 (Red). As shown in A and D. D, surface localization of the GluR2 subunit of the AMPA receptor complex was increased by 39% in the CA1 region of the KO males, but this increase was eliminated in the DCP-LA-treated mice (n = 6). HOECHST33342 labeling (blue) identifiediesd the nuclei in the cellular layers of the CA1 region. (A, B, and C) A trend of increase in surface GluR2 was observed in the CA3 region (but not DG) and neonatal DCP-LA treatment eliminated this trend.

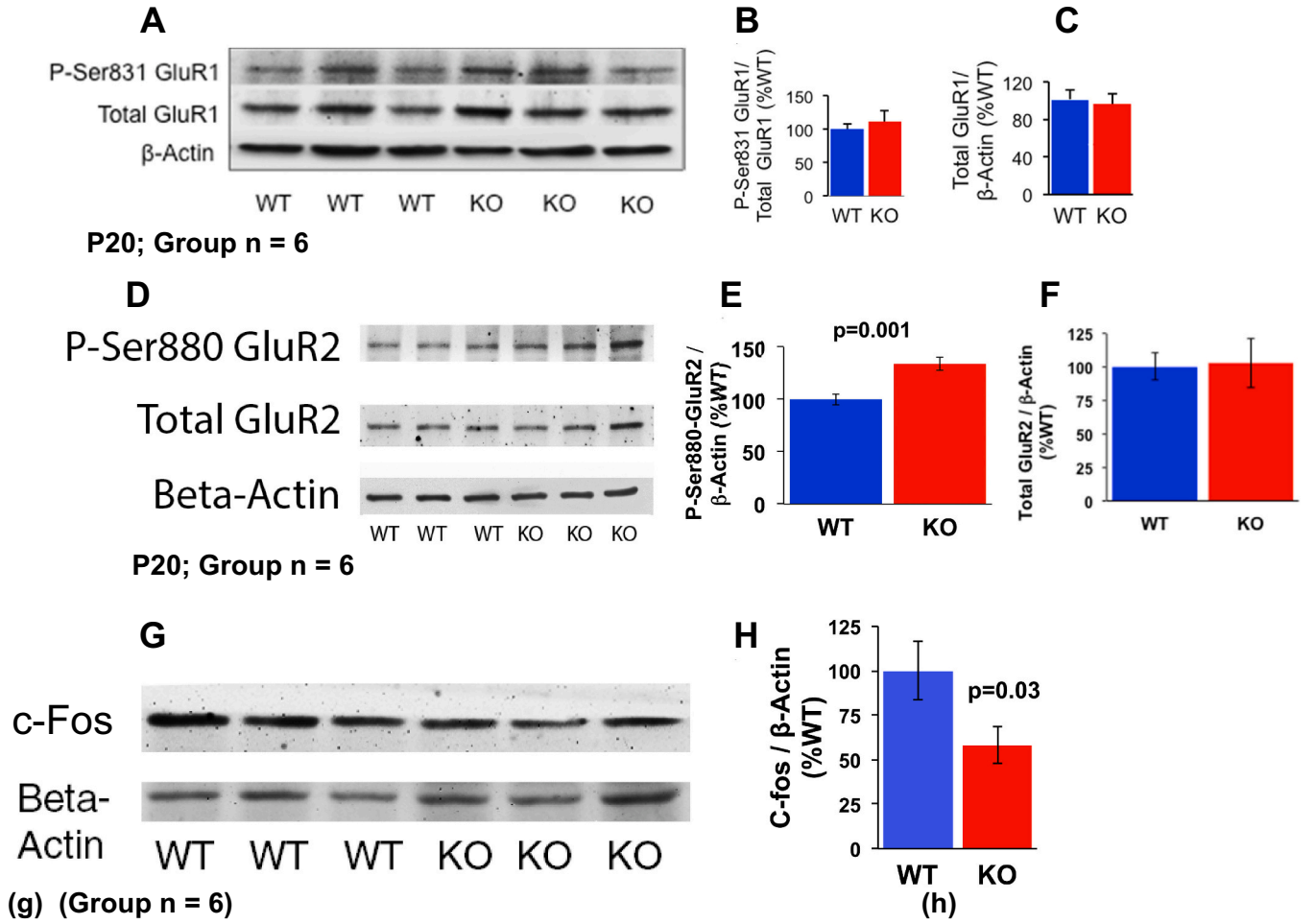


Fig. 4. No change in P-Ser831-GluR1 levels in the PVN, but increased P-Ser880-GluR2 levels and suppressed c-Fos expression indicate inhibited activity in the PVN in P20 KO mice relative to WT. Lysates of PVN tissue obtained from WT and KO males were subjected to Western blot analysis for P-Ser831-GluR1 (A, B), total GluR1 (A, C); P-Ser880-GluR2 (D, E), total GluR2 (D, F), and c-Fos (G, H). Each blot was finally probed for β-actin to normalize for loading. Normalized band intensities were obtained, quantified and compared between WT and KO using six mice in each group (n = 6 per genotype). Western blotting also confirmed a small (17%) but significant suppression of PKCε in the PVN neurons at P20 (Fig. S4).

was used to quantify OXT positive cells within the PVN. We found that the number of OXT-positive cells was suppressed by 25% in the *Fmr1* KO PVN compared with the WT group (Fig. 5A). This deficit was not due to a general loss of PVN neurons, because the HOECHST+ PVN cell number remained comparable between the two groups (Fig. 5C).

To confirm whether OXT expression was PKCε dependent, we systemically treated *Fmr1* KO pups at P6, P10, and P14 with either (1) the selective PKCε activator, DCP-LA, or (2) a cocktail of DCP-LA and the selective PKCε inhibitor, Myr-εV1/2 [25]. To ensure brain entry of Myr-εV1/2, we also intranasally delivered the inhibitor (see Materials and methods). As expected, we found that DCP-LA treatment alone was sufficient to fully normalize the number of OXT-positive cells in the Fmr1 KO PVN to WT levels (Fig. 5A, third column from left). In contrast, when DCP-LA was administered alongside the PKCε inhibitor Myr-εV1/2, OXT expression was further suppressed compared with vehicle-treated KO controls (Fig. 5A, fourth column from left). Both of these changes occurred without any changes in the total number of PVN cells (Fig. 5C), indicating that the process of OXT expression itself was altered. Based on this collective evidence, OXT expression within the PVN at P20 appeared to be dependent on prior PKCε signaling during the early stages of neonatal development (P6-14).

3.4. Pharmacological stimulation of PKCε during the neonatal stage corrects hyper-anxiety and social behavior deficits in adult male Fmr1 KO mice

We have obtained data indicative of reduced PVN OXT expression in the juvenile (P20) *Fmr1* KO mouse brain. We hypothesized that this reduction could be due to increased inhibitory drive exerted on the PVN by the Fmr1 KO hippocampus. This in turn could likely be traced back to reduced PKCε expression in the CA1 area of the ventral hippocampus, which in turn is associated with aberrant AMPA receptor trafficking during the juvenile developmental period (P18). These changes begin early in development, and may lead to more permanent consequences on downstream OXT dependent circuits involved in behavior, particularly anxiety and social behavior. A growing body of work has shown that early postnatal levels of OXT are crucial for normal later-life social behavior [43–45]. If our hypothesis is correct, then social and emotional aberrances in adult *Fmr1* KO mice could potentially be rescued by neonatal PKCε stimulation. To test this hypothesis, we treated *Fmr1* KO pups with either vehicle or 3 mg/kg DCP-LA at P6, P10, and P14 and then assessed anxiety and social behavior in adulthood (2 months of age). Unlike the studies previously outlined here, for these behavioral experiments we treated both male and female pups to determine if DCP-LA would exert a behavioral effect on the generally asymptomatic KO females.

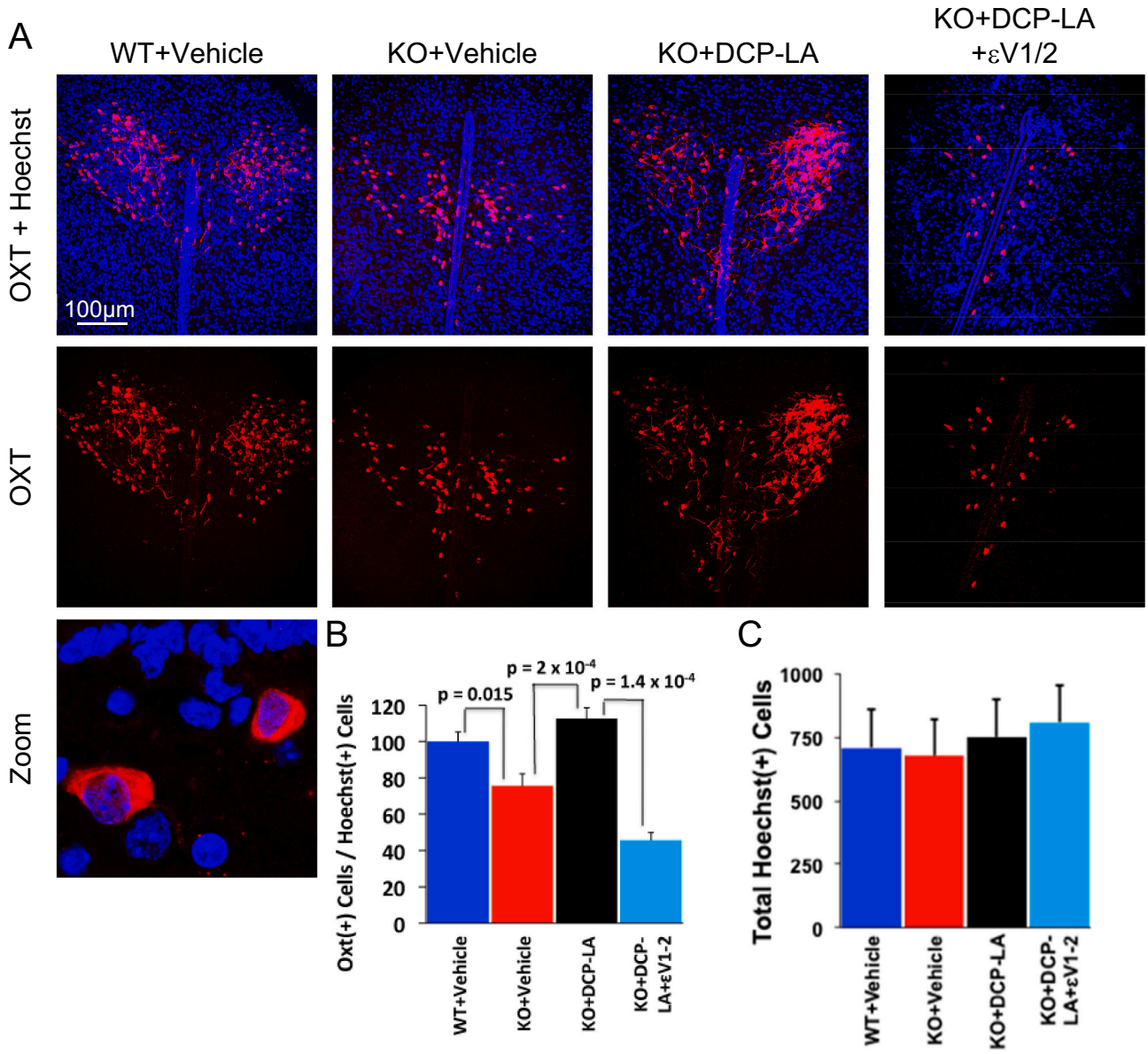


Fig. 5. Decreased oxytocin+ neurons in the PVN of the *Pde6b*^{WT} *Fmr1* KO mice at P20 is corrected in a PKCε-dependent manner by early post-natal DCPLA treatment. (A, B) The number of oxytocin-positive (OXT+) cells was reduced by 25% in the hypothalamic PVN of *Fmr1* KO mice at P20. Neonatal PKCε stimulation by injecting DCP-LA at P6, 10, and 14 corrected the suppressed OXT expression, while a selective PKCε inhibitor eliminates the effect of DCP-LA. (C) The total number of HOECHST+ PVN cells (blue) was comparable across groups (n = 6 per group). A panel in the third row in (A) shows an enlarged view of OXT+ cells confirming the cytoplasmic expression of OXT in the PVN neurons.

Consistent with reports of heightened anxiety disorders in human FXS patients, we observed that in the elevated plus maze (EPM), vehicle-treated Fmr1 KO male mice made significantly less entries into the open arms, and demonstrated a trend of spending less time in the open arms, compared with the vehicle-treated WT males (Fig. 6A and B). In sharp contrast, our homozygous *Fmr1* KO females behaved comparably to the WT females. Furthermore, consistent with our hypothesis, KO males that were treated systemically with DCP-LA from P6-P14 were indistinguishable from WT males, and displayed significantly higher entries into the open arms, and a trend of higher time spent in the open arms, than the vehicle-treated KO males. In contrast, the DCP-LA-treated KO females were statistically indistinguishable from WT and KO females, indicating that DCP-LA had no effect on EPM performance in the KO females. To further confirm that the KO males displayed heightened anxiety, we next performed the light dark (LD) test. Consistent with our observations in the EPM, the KO males spent significantly less time that the WT males in the lit chamber, whereas DCPLA-treated KO males behaved identically to the WT males spending more time in the lit chamber than the vehicle-treated KO males (Fig. S6-1). This indicated a complete rescue of the anxiety phenotype observed in the vehicle-treated KO males in this test. By contrast, both vehicle and DCP-LA treated KO females were statistically indistinguishable from the WT females in the light-dark test (Fig. S6-1). Our results demonstrate that neonatal DCP-LA administration is capable of rescuing anxiety-like behaviors in adult male *Fmr1* KO mice in these tests. Moreover, this treatment did not seem to exert any negative effect on the anxiety phenotype in the asymptomatic *Fmr1* KO females.

We next questioned whether the same neonatal DCP-LA regimen was capable of rescuing social behavior deficits in our Fmr1 KO mice. To this end, we performed the three-chamber social interaction (SI) test. Consistent with human FXS patients, we observed noticeable social behavior deficits in our vehicle-treated *Fmr1* KO male mice, which

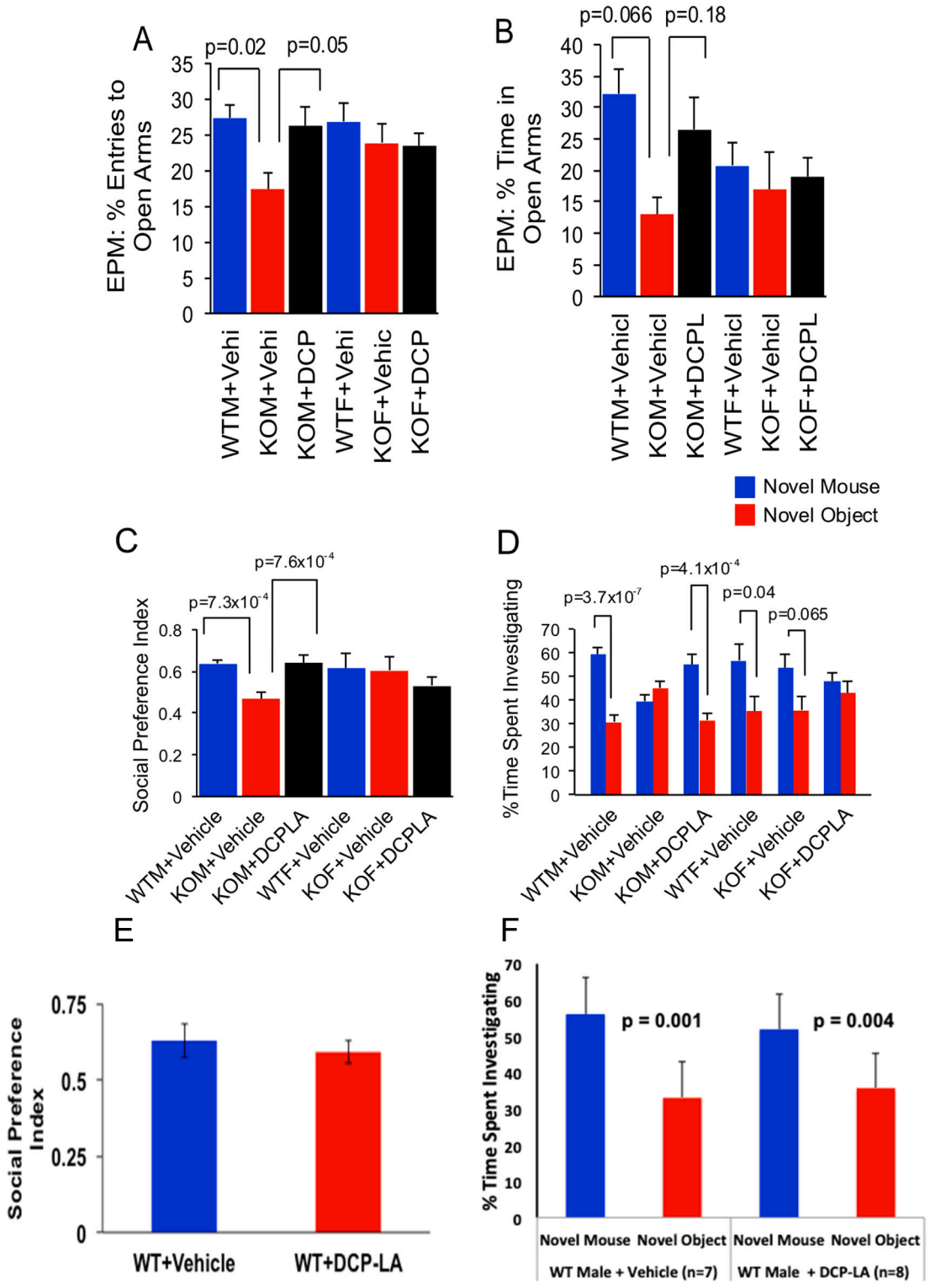


Fig. 6. Neonatal DCP-LA treatment rescues male-specific anxiety behavior and social behavior deficits in visually intact, adult *Pde6b*^{WT} *Fmr1* KO mice in the elevated plus maze (EPM). (A, B) In anxiety behavior, male *FVBPde6b*^{WT} *Fmr1* KO mice (KOM) made significantly less entries into and spent less time in the open arms compared with wild-type *Pde6b*^{WT} males (WTM), but this is corrected with administration of 3 mg/kg DCP-LA at P6, P10, and P14. KO females (KOF) do not differ significantly from WT females (WTF), and neonatal DCP-LA treatment has no effect on anxiety behavior in the KO females. (C, D) Adult *Fmr1* KO males (KOM), but not females (KOF), displayed lack of a preference for the novel mouse over a novel object in the three-chambered social interaction test (SI). In the KO females, neonatal DCPLA treatment impaired social preference for novel mouse (n = 12–14). (E, F) Neonatal DCPLA treatment of WT males did not cause any change in their social preference for the novel mouse. Social preference index = time spent with novel mouse/(time spent with novel mouse + time spent with novel object). Furthermore, compared with the WT controls, the adult KO males but not females displayed a significant increase in anxiety even in the Light-Dark (SD) chamber analysis and this behavior was corrected upon DCP-LA treatment at P6, P10, and P14 (Fig. S6-1). The WT, vehicle or DCP-LA groups of mice showed no significant difference in locomotion in the open field (Fig. S6-2).

lacked a preference for age- and sex-matched novel mouse *versus* a novel object (Fig. 6C and D). However, this deficit was fully corrected in DCP-LA-treated KO males, which, similar to the WT males, spent significantly more time investigating the novel mouse than the novel object. Whereas, the WT control females spent a significantly greater amount of time investigating the novel mouse than the novel object, the vehicle-treated KO females displayed a trend toward spending more time with the novel mouse that was approaching significance. Curiously, we found that neonatal DCP-LA treatment caused the *Fmr1* KO females to spend equivalent amounts of time investigating the novel mouse and novel object (Fig. 6D). This observation is coherent with a recent report that in females but not males, OXT receptors in the BNST appear to stimulate social avoidance in mice in response to social stress, possibly explaining our observations [46]. In our control experiment, we observed no effect of neonatal DCP-LA treatment on social behavior in our WT males (Fig. 6E and F). Nevertheless, these results demonstrate that DCP-LA treatment appears sufficient and capable of fully reversing hyper-anxiety and social behavior deficits in symptomatic *Fmr1* KO males.

To ensure that our results from the EPM, light-dark, and social interaction tests were not influenced by differences in locomotor activity, we lastly performed the open field test on these mice. We detected no statistically significant differences in distance traveled or time spent mobile between any of the groups tested (Fig. S6-2A and B), indicating that our reported effects of neonatal DCP-LA treatment on EPM, light-dark, and social interaction test performance were not due to altered locomotor activity, and thus could be attributed to anxiolytic effects.

To evaluate the effective therapeutic window of DCP-LA treatment, we next conducted an experiment comparing the effect of DCP-LA treatment on P10 and P14 with that from treatment at P6, P10, P14 on adult social behavior. Whereas the best corrective effect was observed when the DCPL-LA treatment started at P6, DCP-LA treatment at P10 and P14 also yielded a significant but lesser correction of social behavior in the KO male mice toward a preference for the novel mouse over a novel object (Fig. 7). By contrast, DCP-LA treatment only at P14 was ineffective in correcting the autistic-like social behavior deficits in these mice (data not shown here).

To confirm that the observed heightened anxiety in the Fmrp-deficient males and the likely involvement of PKCε were not specific for the strain *FVBPde*^{WT}, we also tested WT and *Fmr1* KO males of the strain *FVB/NJ*. We observed that *Fmr1* KO males of this strain also displayed heightened anxiety in EPM and this phenotype was corrected in mice treated neonatally (P6, P10, and P14) with 3 mg/kg of DCP-LA (Fig. S7-1A and B).

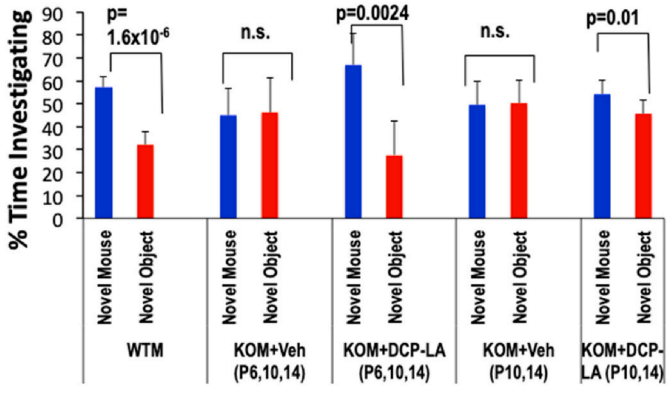


Fig. 7. Early correction of PKCε signaling is essential for the rescue of social behavior. Neonatal treatment of FVB*Pde6b*^{WT}*Fmr1KO* males at P6, 10, 14 with DCP-LA corrected their social behavior to the *Pde6bFmr1*^{WT} levels. A similar treatment starting from P10 (treated on P10 and P14) caused only partial correction of the social behavior of the KOM mice. $n = 7$ (WTM); 5 (KOM + Vehicle (P6, 10, 14)); 5 (KOM+DCPLA (P6, 10, 14)); 7 (KOM + Vehicle (P10, 14)); 8 (KOM + DCPLA (P10, 14)). Lack of *Fmr1* expression in adult male mice of the strain FVB/NJ was also associated with heightened anxiety relative to the FVB/NJ WT males in the EPM test and this aberrance was corrected upon DCP-LA treatment at P6, P10, and P14 (Fig. S7).

4. Discussion

Fragile X Syndrome (FXS) is a heritable genetic disorder that is one of the leading causes of monogenic autism [47]. Currently, no direct cure for FXS exists, and treatment strategies have significant disadvantages. Here, we introduce the possibility of an early-intervention strategy for the treatment of FXS. It has been widely accepted that developmental disorders like autism and FXS involve aberrant brain development during early postnatal stages, which is highly difficult or almost impossible to correct in adulthood. We propose that early intervention can redirect brain development onto the normal path, mitigating these symptoms before they fully develop.

Using the well-established FVB*Pde*^{WT}*Fmr1* KO mouse model of FXS, we have studied a likely Fmrp target, PKCε, in the stimulation of the ventral hippocampal neurons and the regulation of the oxytocinergic neurons in the PVN during the postnatal days 18–20. Our prior studies demonstrated that PKCε is abundantly expressed during early postnatal hippocampal maturation [30]. Although it has been reported that PKCε mRNA is a binding partner of Fmrp [21], it was unclear if PKCε expression was affected in individuals with FXS. Here, we report that in the behaviorally-affected male *Fmr1* KO mice, PKCε is significantly under-expressed in two key areas relevant to social and emotional behavior: the ventral hippocampal CA1 region; and the hypothalamic PVN. In our attempts to elucidate the consequences of this under-expression, we discovered that PKCε deficiency at P18 coincides with increased surface localization of GluR2-containing AMPA receptors in the ventral hippocampus. This is significant because hippocampal responses to sensory stimuli are greatly dependent on AMPA receptor externalization, and any changes to this process can upset the critical balance of excitation and inhibition in the hippocampal circuitry. Interestingly, these findings are consistent with an independent study that has reported heightened hippocampal excitability in *Fmr1* KO mice at this age [48]. Such observations may help explain, at least partially, heightened network excitability in FXS [39], and the fact that many children with FXS are more susceptible to seizures.

What are the potential global consequences of surface accumulation of GluR2 and net hyperexcitability in the FXS hippocampus? Altered responses to excitatory signals in Fmr1 KO CA1 neurons may lead to aberrant synapse formation between the hippocampus and its efferent targets during brain wiring. Because a high proportion of patients with FXS suffer from anxiety disorders, especially social anxiety [39], we studied the integrity of the central oxytocinergic system in FXS, as a downstream target of ventral hippocampal regulation. The major source of OXT in the brain is the PVN of the hypothalamus. Ventral hippocampal neurons are known to project to and activate GABA-ergic neurons of the BNST, which in turn inhibit the PVN neurons [41,42]. We speculate that in the neonatal *Fmr1* KO brain, CA1 neurons may be hyper-responsive to incoming excitatory signals, and in turn exert increased inhibitory drive upon the PVN, potentially suppressing OXT production. We report that at P20, *Fmr1* KO mice display a reduced number of OXT+ cells in the PVN compared with WT controls. Moreover, we observe that OXT expression in the juvenile PVN is PKCε-dependent, since neonatally DCP-LA treated KOs displayed normal levels of OXT+ cells in the PVN at P20, whereas simultaneous PKCε inhibition further suppresses this number. However, mechanistically, how exactly PKCε regulates OXT synthesis within PVN neurons needs further investigation. As discussed earlier, the ventral hippocampus is known to tonically inhibit parvocellular PVN activity [49]. Furthermore, projections from the ventral subiculum (a major source of hippocampal efferents to the hypothalamus) also contact GABA-ergic neurons in the BNST, medial pre-optic area, and hypothalamic nuclei, which in turn project to the PVN [50]. Additionally, activation of

pyramidal neurons in the CA1 region of the ventral hippocampus, which project heavily to the subiculum, has been shown to produce anxiety-like behavior in rodents [51,52], possibly by suppressing central OXT signaling at its root, within the PVN. Consistently, lesions to the ventral hippocampus produce an anxiolytic effect [31,32].

Despite such possibilities, the mechanistic link between PKCε and OXT expression in the PVN is rendered complex by two findings (1) the DCP-LA treatment needs to be started at P6 to observe the complete correction of behavior in the KO mice in adulthood (Fig. 7), and (2) DCP-LA treatment at P6, P10, P14 causes the observed correction of OXT expression in the PVN at P20 (Fig. 5), and only one DCP-LA treatment at P18 does not correct the stunted OXT expression at P20 in the KO males (unpublished data). Further complicating the investigation, PKCε expression in the CA1 region of the ventral hippocampus did not appear to be suppressed at P6 in the KO males (Fig. S1-2). This may mean that the PKCε signaling, rather than the observed suppression of PKCε in hippocampus of the P18 KO males, might be impaired from the early stages, thereby culminating in the significant stunting of OXT expression in PVN at P20. Thus, rather than being directly linked to the suppression of PKCε at P18, the suppressed phosphorylation of GluR2 could be a prolonged neonatal effect of the absence of Fmrp. Only such persistent effect may be linked to the stunted OXT expression by the PVN neurons at P20 in the KO mice. Further studies are required to test this hypothesis.

How would the stunted OXT expression in the P20 PVN affect social behavior in the KO mice? It has been reported that a subset of parvocellular neurons within the PVN of the hypothalamus regulates social behavior by radiating oxytocinergic projections to the nucleus accumbens (NAcc) region of the basal forebrain [53,54]. In their study, Dölen and coworkers show that OXT released by the oxytocinergic neurons binds to OXT receptors on the raphé neurons, thereby stimulating serotonin (5-HT) release from these neurons at their synapses in the nucleus accumbens (NAcc). The released 5-HT molecules bind to inhibitory 5-HT_{1B} receptors on glutamatergic terminals from various brain regions, such as cortex, amygdala, thalamus, that terminate on the medium spiny neurons of the NAcc. This causes OXT-induced LTD in the NAcc, which in turn is linked to the reinforcing properties of social interaction in mice [53].

It is known that FXS females typically display milder symptoms than male patients. This is attributed to the fact that all human females with the full mutation are heterozygous, because the full mutation can only be transmitted maternally. Consequently, due to lyonization, all full mutation females are mosaics for activity of the affected X chromosome [55–58]. Thus, it is presumed that tissue-specific skewed X inactivation may underlie the variability of FXS in women. However, the female KO mice used in this study were homozygous for the Fmr1 KO mutation, and therefore, the reason for the sex-specific effect of Fmr1 knockout on anxiety and social interaction profiles remains to be understood.

This study introduces early postnatal PKCε-mediated signaling as a likely regulator of brain wiring, in regards to social and anxiety behavior. For the first time, we have provided evidence that PKCε expression and its signaling are aberrant in the *Fmr1* KO hippocampus. Furthermore, we show that OXT expression in the PVN neurons is stunted in the *Fmr1* KO mice at P20. We demonstrate that through early intervention, using a highly selective stimulator of PKCε, it is possible to correct the OXT expression at P20 and the later-life social behavior deficits and hyper anxiety in a leading FXS mouse model. Such observations set the stage for the exploration of possible mechanisms by which this rescue takes place. This work also submits the possibility that early intervention using PKCε activators may serve as a promising therapeutic strategy for FXS.

CRediT authorship contribution statement

Alexandra Emma Marsillo: Conducted experiments, analyzed data, participated in writing the manuscript. *Lovena David*: Conducted experiments, analyzed data, read and edited manuscript. *Bishoy Gerges*: Conducted experiments, analyzed data, assisted in preparing figures. *Daniel Kerr*: Participated in curating and analyzing data and in writing and revising the manuscript. *Vitaliy Lasiychuk*: Conducted experiments, re-confirmed experimental data, and prepared figures. *Rodina Sadek*: Conducted behavioral experiments, analyzed data, and participated in preparing figures. *David Salame*: Conducted behavioral experiments, analyzed data, and participated in preparing figures. *Youstina Soliman*: Conducted behavioral experiments, analyzed data, and participated in preparing figures. *Silvia Menkes*: Analyzed data, and participated in preparing figures. *Aheli Chatterjee*: Analyzed data, and participated in preparing figures. *Andrew Mancuso*: Analyzed data, and participated in preparing figures. *Probal Banerjee*: Conceptualized and coordinated the project, analyzed and curated data, wrote and edited the manuscript.

Declaration of competing interest

Dr. Probal Banerjee has recently submitted a Provisional patent application entitled “Use of DCPLA as a Therapeutic Agent for Fragile X Syndrome and Autism” (Application No.: 62/690,224). The other authors do not have any conflict of interest.

Acknowledgments

This study was funded by the FRAXA Research Foundation. Alexandra Marsillo and Andrew Mancuso received fellowship and tuition support from the CUNY Graduate Center and teaching assistantships from the departments of Biology and Chemistry, respectively, at the College of Staten Island. The authors are grateful to Drs. Daniel McCloskey, Carl Dobkin, Kathryn Chadman for helpful discussions.

Appendix A. Supplementary data

Supplementary data to this article can be found online at https://doi.org/10.1016/j.bbadis.2020.166048.

References

[1] A.L. Ludwig, G.M. Espinal, D.I. Pretto, A.L. Jamal, G. Arque, F. Tassone, R. F. Berman, P.J. Hagerman, CNS expression of murine fragile X protein (FMRP) as a function of CGG-repeat size, Hum. Mol. Genet. 23 (2014) 3228–3238.
[2] A.J. Verkerk, M. Pieretti, J.S. Sutcliffe, Y.H. Fu, D.P. Kuhl, A. Pizzuti, O. Renier, S. Richards, M.F. Victoria, F.P. Zhang, Identification of a gene (FMR-1) containing a CGG repeat coincident with a breakpoint cluster region exhibiting length variation in fragile X syndrome, Cell 65 (1991) 905–914.
[3] B.E. Pfeiffer, K.M. Huber, The state of synapses in fragile X syndrome, Neuroscientist 15 (2009) 549–567.
[4] J. Tolmie, Fragile X syndrome - diagnosis, treatment and research, J. Med. Genet. 39 (2002) 783.
[5] W.E. Kaufmann, M.T. Abrams, W. Chen, A.L. Reiss, Genotype, molecular phenotype, and cognitive phenotype: correlations in fragile X syndrome, Am. J. Med. Genet. 83 (1999) 286–295.
[6] M.R. Santoro, S.M. Bray, S.T. Warren, Molecular mechanisms of fragile X syndrome: a twenty-year perspective, Annual Review of Pathology: Mechanisms of Disease 7 (2012) 219–245.
[7] E. Berry-Kravis, V. Des Portes, R. Hagerman, S. Jacquemont, P. Charles, J. Visootsak, M. Brinkman, K. Rerat, B. Koumaras, L. Zhu, G.M. Barth, T. Jaecklin, G. Apostol, F.V. Raison, Mavoglurant in fragile X syndrome: results of two randomized, double-blind, placebo-controlled trials, Science Translational Medicine 8 (2016), 321ra325-321ra325.
[8] R. Bailey Jr., M. D.B., M. Olmsted, D.B. Holiday, Co-occurring conditions associated with FMR1gene variations: findings from a national parent survey, Am J. Med. Genet A 146A (2008) 2060–2069.
[9] L. Cordeiro, E. Ballinger, R. Hagerman, D. Hessl, Clinical assessment of DSM-IV anxiety disorders in fragile X syndrome: prevalence and characterization, J. Neurodevelop Disord 3 (2011) 57–67.
[10] D.B. Budimirovic, W.E. Kaufmann, What can we learn about autism from studying fragile X syndrome? Developmental Neurosceince 33 (2011) 379–394.
[11] M.R. Tranfaglia, The psychiatric presentation of fragile X: evolution of the diagnosis and treatment of the psychiatric comorbidities of fragile X syndrome, Developmental Neurosceince 33 (2011) 337–348.
[12] I.D. Neumann, D.A. Slattery, Oxytocin in general anxiety and social fear: a translational approach, Biol. Psychiatry 79 (2016) 213–221.

[13] S.S. Hall, A.A. Lightbody, B.E. McCarthy, K.J. Parker, A.L. Reiss, Effects of intranasal oxytocin on social anxiety in males with fragile X syndrome, Psychoneuroendocrinology 37 (2012) 509–518.
[14] G. Leng, M. Ludwig, Intranasal oxytocin: myths and delusions, Biol. Psychiatry 79 (2016) 243–250.
[15] E. Anagnostou, L. Soorya, W. Chaplin, J. Bartz, D. Halpern, S. Wasserman, A. T. Wang, L. Pepa, N. Tanel, A. Kushki, E. Hollander, Intranasal oxytocin versus placebo in the treatment of adults with autism spectrum disorders: a randomized controlled trial, Molecular Autism 3 (2012) 16.
[16] M.R. Dadds, E. MacDonald, A. Cauchi, K. Williams, F. Levy, J. Brennan, Nasal oxytocin for social deficits in childhood autism: a randomized controlled trial, J. Autism Dev. Disord. 44 (2014) 521–531.
[17] A.J. Guastella, K.M. Gray, N.J. Rinehart, G.A. Alvares, B.J. Tonge, I.B. Hickie, C. M. Keating, C. Cacciotti-Saija, S.L. Einfeld, The effects of a course of intranasal oxytocin on social behaviors in youth diagnosed with autism spectrum disorders: a randomized controlled trial, J. Child Psychol. Psychiatry 56 (2015) 444–452.
[18] A. Contractor, V.A. Klyachko, C. Portera-Cailliau, Altered neuronal and circuit excitability in fragile X syndrome, Neuron 87 (2015) 699–715.
[19] E. Berry-Kravis, Epilepsy in fragile X syndrome, Dev. Med. Child Neurol. 44 (2002) 724–728.
[20] G. Incorpora, G. Sorge, A. Sorge, L. Pavone, Epilepsy in fragile X syndrome, Brain Dev. 24 (2002) 766.
[21] J.C. Darnell, S.J. van Driesche, C. Zhang, K.Y.S. Hung, A. Mele, C.E. Fraser, E. F. Stone, C. Chen, J.J. Fak, S.W. Chi, D.D. Licatalosi, J.D. Richter, R.B. Darnell, FMRP stalls ribosomal translocation on mRNAs linked to synaptic function and autism, Cell 146 (2011) 247–261.
[22] M.-K. Sun, J. Hongpaisan, D.L. Alkon, Rescue of synaptic phenotypes and spatial memory in young fragile X mice, J. Pharmacol. Exp. Ther. 357 (2016) 300–310.
[23] M.-K. Sun, D.L. Alkon, Bryostatin-1: pharmacology and therepeutic potential as a CNS drug, CNS Drug Reviews 12 (2006) 1–8.
[24] T. Nishizaki, A. Tanaka, Pkc-epsilon Activator vol. PCT/JP2011/076302, Nishizaki Bioinformation Research Institute, Kobe-shi (JP), U.S.A., 2013, p. 3.
[25] S. Samaddar, B. Ranasinghe, S.J. Tantry, P.R. Debata, P. Banerjee, Involvement of vascular endothelial growth factor in serotonin 1A receptor-mediated neuroproliferation in neonatal mouse hippcampus, Adv. Exp. Med. Biol. 842 (2015) 375–388.
[26] S. Mukherjee, J.N.E. Baidoo, A. Fried, D. Atwi, S. Dolai, J. Boockvar, M. Symons, R. Ruggieri, K. Raja, P. Banerjee, Curcumin changes the polarity of tumor-associated microglia and eliminates glioblastoma, Int. J. Cancer 139 (2016) 2838–2849.
[27] D.J. Kerr, A. Marsillo, S.R. Guariglia, T. Budylin, R. Sadek, Menkes, A. Chauhan, G. Y. Wen, D.P. McCloskey, A.J. Wieraszko, P. Banerjee, Aberrant hippocampal Atp8a1 levels are associated with altered synaptic strength, electrical activity, and autistic-like behavior, Biochimica et Biophysica Acta (Molecular Basis of Disease) 1862 (2016) 1755–1765.
[28] I. Song, R.L. Huganir, Regulation of AMPA receptors during synaptic plasticity, Trends in Neuroscience 25 (2002) 578–588.
[29] H.J. Chung, J. Xia, R.H. Scannevin, X. Zhang, R.L. Huganir, Phosphorylation of the AMPA receptor subunit GluR2 differentially regulates its interaction with PDZ domain-containing proteins, The Journal of Neuroscience 20 (2000) 7258–7267.
[30] S. Purkayastha, S.S. Fernando, S. Diallo, L. Cohen, K. Levano, P. Banerjee, Regulation of protein kinase C isozymes during early post-natal hippocampal development, Brain Res. 1288 (2009) 29–41.
[31] D.M. Bannerman, J.N.P. Rawlings, S.B. McHuch, R.M.J. Deacon, B.K. Yee, T. Bast, W.N. Zhang, H.H.J. Pothuizen, J. Feldon, Regional dissociations within the hippocampus—memory and anxiety, Neurosci. Biobehav. Rev. 28 (2004) 273–283.
[32] K.G. Kjelstrup, F.A. Tuvnes, H.-A. Steffenach, R. Murison, E.I. Moser, M.B. Moser, Reduced fear expression after lesions of the ventral hippocampus, Proc. Natl. Acad. Sci. U. S. A. 99 (2002) 10825–10830.
[33] J.P. Herman, O. Eyigor, D.R. Ziegler, L. Jennes, Expression of ionotropic glutamate receptor subunit mRNAs in the hypothalamic paraventricular nucleus of the rat, J. Comp. Neurol. 422 (2000) 352–362.
[34] M.A. Jenkins, S.F. Traynelis, PKC phosphorylates GluA1-Ser831 to enhance AMPA receptor conductance, Channels 6 (2012) 60–64.
[35] V. Derkach, A. Barria, T.R. Soderling, Ca(2+)/calmodulin-kinase II enhances channel conductance of α-amino-3-hydroxy-5-methyl-4-isoxazolepropionate type glutamate receptors, Proc. Natl. Acad. Sci. U. S. A. 96 (1999) 3269–3274.
[36] H.-J. Lee, A.H. Macbeth, J. Pagani, W.S. Young 3rd, Oxytocin: the great facilitator of life, Prog. Neurobiol. 88 (2009) 127–151.
[37] C.J. Yatawara, S.L. Einfeld, I.B. Hickie, T.A. Davenport, A.J. Guastella, The effect of oxytocin nasal spray on social interaction deficits observed in young children with autism: a randomized clinical crossover trial, Mol. Psychiatry 21 (2016) 1225–1231.
[38] M. Yoshida, Y. Takayanagi, K. Inoue, T. Kimura, L.J. Young, T. Onaka, K. Nishimori, Evidence that oxytocin exerts anxiolytic effects via oxytocin receptor expressed in serotonergic neurons in mice, J. Neurosci. 29 (2009) 2259–2271.
[39] A. Contractor, V. Klyachko, C. Portera-Cailliau, Altered neuronal and circuit excitability in fragile X syndrome, Neuron 87 (2015) 699–715.
[40] O. Penagarikano, M.T. Lazaro, X.-H. Lu, A. Gordon, H. Dong, H.S. Lam, E. Pales, N. R. Maidment, N.P. Murphy, W. Yang, P. Golshani, D.H. Geshwind, Exogenous and evoked oxytocin restores social behavior in the Cntnap2 mouse model of autism, Sci. Transl. Med. 7 (2015) 1–11.
[41] J.P. Herman, J.M. McKlveen, S. Ghosal, B. Kopp, A. Wulsin, R. Makinson, J. Scheimann, B. Myers, Regulation of the hypothalamic-pituitary-adrenocortical stress response, Comprehensive Physiology 6 (2016) 603–621.
[42] S.M. Smith, W.W. Vale, The role of the hypothalamic-pituitary-adrenal axis in neuroendocrine responses to stress, Dialogues Clin. Neurosci. 8 (2006) 383–395.
[43] V. Grinevich, M.G. Desarmenien, B. Chini, M. Tauber, F. Muscatelli, Ontogenesis of oxytocin pathways in the mammalian brain: late maturation and psychosocial disorders, Front. Neuroanat. 8 (2014) 1–18.
[44] E.A.D. Hammock, Developmental perspectives on oxytocin and vasopressin, Neuropsychopharmacol. Rev. 40 (2015) 24–42.
[45] T.V. Miller, J.K. Caldwell, Oxytocin during development: possible organizational effects on behavior, Frontiers in Endocrinology 6 (2015) (Article 76).
[46] N. Duque-Wilckens, M.Q. Steinman, M. Busnelli, B. Chini, S. Yokoyama, M. Pham, S.A. Laredo, R. Qao, A. Perkeybile, V.A. Minie, P.B. Tan, K.K. Bales, B.C. Trainor, Oxytocin receptors in the anteromedial bed nucleus of the stria terminalis promote stress-induced social avoidance in female California mice, Biol. Psychiatry 83 (2018) 203–213.
[47] R. Dahlhaus, Of men and mice: modeling the fragile X syndrome, Front. Mol. Neurosci. 11 (2018) 1–38.
[48] S.-C. Chuang, W. Zhao, R. Bauchwitz, Q. Yan, R. Bianchi, R.K.S. Wong, Prolonged epileptiform discharges induced by altered group I metabotropic glutamate receptor-mediated synaptic responses in hippocampal slices of a fragile X mouse model, J. Neurosci. 25 (2005) 8048–8055.
[49] J.P. Herman, W.E. Cullinan, E.A. Young, H. Akil, S.J. Watson, Selective forebrain fiber tract lesions implicate ventral hippocampal structures in tonic regulation of paraventricular nucleus corticotropin-releasing hormone (CRH) and arginine vasopressin (AVP) mRNA expression, Brain Res. 592 (1992) 228–238.
[50] F. Herman, H. J.P., N.K. Mueller, Y. Ulrich-Lai, M.M. Ostrander, D.C. Choi, W. E. Cullinan, Central mechanisms of stress integration: hierarchical circuitry controlling hypothalamo–pituitary–adrenocortical responsiveness, Frontiers in Neuroendocrinology 24 (2003) 151–180.
[51] A. Degroot, D. Treit, Anxiety is functionally segregated within the septo-hippocampal system, Brain Res. 1001 (2004) 60–71.
[52] A.C. Felix-Ortiz, A. Beyeler, C. Seo, C.A. Leppla, C.P. Wildes, K.M. Tye, BLA to vHPC inputs modulate anxiety-related behaviors, Neuron 79 (2013) 658–664.
[53] G. Dolen, A. Darvishzadeh, K.W. Huang, R.C. Malenka, Social reward requires coordinated activity of nucleus accumbens oxytocin and serotonin, Nature 501 (2013) 179–184.
[54] G. Dölen, R.C. Malenka, The emerging role of nucleus accumbens oxytocin in social cognition, Biol. Psychiatry 76 (2014) 354–355.
[55] C.S. Dobkin, S.L. Nolin, I. Cohen, V. Sudhalter, M.D. Bialer, X.H. Ding, E.C. Jenkins, N. Zhong, W.T. Brown, Tissue differences in fragile X mosaics: mosaicism in blood cells may differ greatly from skin, Am. J. Med. Genet. 64 (1996) 296–301.
[56] P. Jin, S.T. Warren, Understanding the molecular basis of fragile X syndrome, Human Moleculear Genetics 9 (2000) 901–908.
[57] S.T. Warren, S.L. Sherman, The Fragile X Syndrome, 8th edition, McGraw-Hill, New York, NY, 2000.
[58] D. Wöhrle, M.C. Hirst, I. Kennerknecht, K.E. Davies, P. Steinbach, Genotype mosaicism in fragile X fetal tissues, Hum. Genet. 89 (1992) 114–116.